



Published in final edited form as:

*Cancer Res.* 2011 April 15; 71(8): 3152–3161. doi:10.1158/0008-5472.CAN-10-3543.

## Cancer-Associated Loss-of-Function Mutations Implicate DAPK3 as a Tumor Suppressing Kinase

John Brognard<sup>1,2</sup>, You-Wei Zhang<sup>2,3</sup>, Lorena A. Puto<sup>2</sup>, and Tony Hunter<sup>2</sup>

<sup>1</sup> Signalling Networks in Cancer Group, Cancer Research UK, Paterson Institute for Cancer Research, The University of Manchester, Manchester, UK

<sup>2</sup> Molecular and Cellular Biology Laboratory, The Salk Institute, La Jolla, California, USA

### Abstract

Cancer kinome sequencing studies have identified several protein kinases predicted to possess driver (i.e. causal) mutations. Using bioinformatic applications we have pinpointed DAPK3 (ZIPK) as a novel cancer-associated kinase with functional mutations. Evaluation of nonsynonymous point mutations, discovered in DAPK3 in various tumors (T112M, D161N, and P216S), reveals that all three mutations decrease or abolish kinase activity. Furthermore, phenotypic assays indicate that the three mutations observed in cancer abrogate the function of the kinase to regulate both the cell cycle and cell survival. Co-expression of WT and cancer mutant kinases demonstrates that the cancer mutants dominantly inhibit the function of the WT kinase. Reconstitution of a non-small cell lung cancer (NSCLC) cell line that harbors an endogenous mutation in DAPK3 (P216S) with WT DAPK3 resulted in decreased cellular aggregation and increased sensitivity to chemotherapy. Our results suggest that DAPK3 is a tumor suppressor where loss-of-function mutations promote increased cell survival, proliferation, cellular aggregation and increased resistance to chemotherapy.

### Keywords

Tumor Suppressor; Kinase; Cell Cycle; Apoptosis; Dominant Negative

### Introduction

Sequencing technologies are evolving at a rapid rate resulting in decreasing costs associated with sequencing a single genome. Estimates predict the cost of sequencing a single genome will drop significantly and exome sequencing costs are already estimated at \$5000, making it feasible that any cancer patient may soon be able to have both their normal and cancer genomes sequenced (1). Comparison of these genomes will provide a snapshot of the genetic aberrations that occurred during the evolution of a cancer (2,3). While the sequencing of a patient's normal and cancer genome is becoming feasible, our understanding of the many genetic aberrations that contribute to various cancer phenotypes lags far behind the development and application of this technology. If this information is to become clinically relevant we must understand and catalog the functional consequences of the observed genetic changes. Understanding both the functional consequences of genetic

\*Correspondence to: John Brognard (jbrognard@picr.man.ac.uk); Tony Hunter (hunter@salk.edu).

<sup>3</sup>Present address: Department of Pharmacology, Case Western University, 2109 Adelbert Road, Cleveland, OH 44106

The authors declare that there are no conflicts of interest.

changes and the signaling networks they impact will be essential if this information is to be used as a guide for therapeutic treatment (4).

In an effort to identify protein kinases with candidate cancer driver mutations, we used bioinformatic tools to analyze kinases with somatic mutations reported in a cancer kinome sequencing study performed by the Sanger Centre that evaluated 518 kinases in 210 cancers (5–8). We identified DAPK3 as a strong candidate to possess functional cancer-associated mutations. DAPK3 (also called ZIPK) is a member of the DAPK (death-associated protein kinase) family (9), and in addition to the N-terminal catalytic domain, this kinase has a leucine zipper domain and two putative NLS (10). DAPK3 is pro-apoptotic (11), and proposed to be a tumor suppressor, suggesting that mutations in DAPK3 could result in loss of function. Consistent with this notion, the gene for DAPK1, which has 83% homology with DAPK3 in the kinase domain (9), is frequently methylated in cancers, and DAPK1 is considered a tumor suppressing kinase (12–14). All three observed cancer mutations in DAPK3 are in residues conserved in the other two DAPK family members, DAPK1 and DAPK2 (Figure 1A). D161 is in the DFG motif, and its mutation to Asn would be expected to greatly reduce catalytic activity; based on the DAPK3 catalytic domain structure (15), T112 is in a surface accessible loop at the start of the C-lobe, and P216 lies in an interhelix loop largely buried in the C-lobe (Figure 1B). The DAPK3 mutations are heterozygous and each cancer patient retains a wild-type (WT) allele. The DAPK3 gene is mutated at a frequency of 3.2% in the panel of lung, ovarian, and colon cancers examined (the frequency of mutations was 1.4% in all cancers examined) (8). The T112M and D161N mutations were identified in the primary tumors of a colon cancer and ovarian cancer patient, respectively, and no DAPK3 mutations were identified in normal cells from the same patients. The P216S mutation was identified in the H1770 NSCLC cell line and no DAPK3 mutations were observed in the pair-matched normal cells (NCI-BL1770 – available through ATCC).

Our results indicate that all three mutations in DAPK3 decrease or abolish the function of the kinase and render it unable to regulate cell cycle progression and cell survival. Furthermore, we observe that the cancer mutants can suppress the function of the WT kinase, suggesting these mutants can act in a dominant-negative fashion. Reconstitution of the DAPK3 pathway in a cancer cell line harboring an endogenous mutation in DAPK3 results in loss of cellular aggregation and increased sensitivity to chemotherapy.

## Materials and Methods

### Materials

DAPK3-specific SMARTpool siRNA was purchased from Dharmacon and targeted the following sequences: 5'-ccacgcgtctgaaggagta-3' (si-1); 5'-gatccaagcggagaatga-3' (si-2); 5'-ggacgtggaggaccattat-3' (si-3); and 5'-gaacgtgcgtggtgaggac-3' (si-4) in DAPK3. Single DAPK3 siRNA targeted the following sequences 5'-acgacatcttcgagaaca-3' (siDAPK3-1), 5'-cagccaagtcatcaagaa-3' (siDAPK3-2), and 5'-acatcatgctggtggacaa-3' (siDAPK3-3). The following phospho-specific antibodies were purchased from Cell Signaling: P-MLC2 (Thr18/Ser19), and P-histone H3 (Thr11). DAPK3 (ZIPK) antibody was purchased from ProSci Incorporated. MLC2 antibody was purchased from Santa Cruz (sc-28329) and anti-FLAG monoclonal antibody was purchased from Sigma (F3165). Propidium iodide and etoposide were both purchased from Sigma. Cell lines were originally purchased from ATCC and were authenticated by the ATCC cell biology program and were not passaged for longer than six months before bringing new cells out of freeze or purchasing a new cell aliquot from the ATCC. The H157 NSCLC cell line was a gift from Dr. Phillip Dennis, National Cancer Institute, and was established at the NCI/Navy Medical oncology.

## Cloning and expression

3X-Flag full-length DAPK3 cDNA, T180A, and  $\Delta 273$  were provided by Dr. Timothy Haystead (Department of Pharmacology and Cancer Biology, Duke University Medical Center, Durham, North Carolina 27710). HA-DAPK3 was provided by Dr. Kevan Shokat (Department of Cellular and Molecular Pharmacology, University of California, San Francisco). The cancer mutant DAPK3 variants were generated by converting the nucleotide at position 335 from a C to a T (T112M); nucleotide at position 481 from a G to an A (D161N); and nucleotide at position 646 from a C to a T (P216S) using QuikChange site directed mutagenesis kit (Stratagene). These variants were identical to the somatic variants observed in cancer patients or in the NSCLC cell line H1770 (P216S). GST-tagged myosin light chain for bacterial expression, used for *in vitro* DAPK3 kinase assays, was a gift from Dr. Ruey-Hwa Chen (Institute of Biological Chemistry, Academia Sinica, Taipei, Taiwan).

## Cell transfections and immunoblotting

The H1770 NSCLC cell line was maintained in RPMI 1640 (Cellgro), and all other cell lines were maintained in DMEM (Cellgro); both media were supplemented with 10% FBS and 1% penicillin/streptomycin. Cells were maintained at 37° C in 5% CO<sub>2</sub>. Transient transfections of all cell types were carried out by using Effectene reagents (Qiagen). Lipofectamine 2000 (Invitrogen) was used to transfect siRNAs into all cells. Transient transfections and siRNA experiments were performed as previously described (29), except for H1770 cells. H1770 cells were pipetted repeatedly to break up cell aggregates and transfected immediately as previously described (29). Transfection efficiencies for 293T and H157 cell lines averaged between 70–90% for each experiment; efficiencies for all other cell lines averaged between 50–80%. For immunoblotting, transfected cells were lysed in Buffer 1 at room temperature (50 mM Na<sub>2</sub>HPO<sub>4</sub>, pH 7.5, 1 mM sodium pyrophosphate, 20 mM NaF, 2 mM EDTA, 2 mM EGTA, 1% SDS, 1 mM DTT, 200  $\mu$ M benzamidine, 40  $\mu$ g ml<sup>-1</sup> leupeptin, and 1 mM PMSF) and sonicated for 4 seconds. Lysates containing equal amounts of protein were analyzed on SDS-PAGE gels, and individual blots were probed using each antibody.

## Kinase assays and co-immunoprecipitations

GST-MLC2 was expressed in BL21 bacterial cells and kinase assays using GST-MLC2 as a substrate were performed using immunoprecipitated FLAG-DAPK3. The activity of full length FLAG-DAPK3 and other indicated variants was assessed by expressing and immunoprecipitating FLAG-DAPK3 from H157 cell lysates. Cells were lysed in Buffer 2 (20 mM HEPES, pH 7.4, 1% Triton X-100, 1 mM DTT, 200  $\mu$ M benzamidine, 40  $\mu$ g ml<sup>-1</sup> leupeptin, 1 mM PMSF), sonicated for 3 seconds, and precleared. Detergent soluble lysates (buffer 2) were incubated overnight at 4° C with FLAG antibody and UltraLink Protein A/G beads (Pierce). Beads were then washed three times with Buffer 1 and incubated in kinase buffer (25 mM Tris (pH 7.5), 5 mM  $\beta$ -glycerophosphate, 2 mM DTT, 0.1 mM Na<sub>3</sub>VO<sub>4</sub>, 10 mM MgCl<sub>2</sub>), and 200  $\mu$ M ATP with purified GST-MLC2, 1  $\mu$ g per reaction in 50  $\mu$ l kinase reaction buffer. Kinase reactions were performed at 30° C for 25 minutes, terminated by the addition of sample buffer and phosphorylation was detected using the P-MLC2 antibody (Thr18/Ser19).

## Proliferation and apoptosis assays

For apoptotic assays, cells were switched to low serum media conditions (0.1% FBS) and transfected with the indicated DAPK3 constructs for 48 hr. Floating cells were collected, and adherent cells were harvested by trypsinization and then centrifuged at 1000 x g for 5 min. Cells were fixed in ice-cold 70% methanol, added drop wise, and then incubated at 20° C for 30 min. Cells were centrifuged and incubated with propidium iodide (25  $\mu$ g/ml)

supplemented with RNase A (30 µg/ml) for 30 min at room temperature. Quantification of sub-2N DNA in apoptosis assays was determined by flow cytometry analysis using a Becton Dickinson FACSort and by manual gating using CellQuest software. Gating was performed on blinded samples. For all cell lines, apoptotic assays were performed on whole cell population. To determine G1/S ratios, cells were transfected with FLAG-DAPK3 constructs and incubated under high serum conditions (10% FBS) for 48 hr. For BrdU incorporation assays, cells were maintained in high growth media (10% FBS) and transfected DAPK3 constructs and incubated for 48 hr prior to performing assays following the manufacturer's protocol (Calbiochem, QIA58). For DAPK3 siRNA-depleted cells, BrdU incorporation assays were performed on cells incubated under low serum conditions (0.1% FBS) and transfected with 100 nM SMARTpool siRNA for 48 hr.

### Statistical and Cell Aggregation Analysis

Statistical comparison of values was performed using the Student t test comparing empty vector controls or untreated cells to indicated DAPK3 constructs. Quantification of cellular aggregation was determined using image J software and spheroid size was correlated to the number of pixels in an area of a given spheroid. Eight cellular aggregates were included in each measurement.

### Results

To determine if mutations identified in DAPK3 are likely to alter the protein function, we used the CanPredict (<http://www.cgl.ucsf.edu/Research/genentech/canpredict/>) web application to determine if the mutations are likely to be cancer-associated mutations (6). This web application employs an algorithm based on three measurements (SIFT, LogR.E-value, and GOSS values) to determine if a given mutation is a probable cancer mutation (6). To demonstrate how this analysis could enhance the selection of potential cancer-associated kinases: evaluation of mutations in DAPK3 by CanPredict reveals that all three somatic mutations are predicted to be cancer-related, and therefore we considered this kinase to be an excellent candidate for further investigation (Figure 1C) (at least one mutation in DAPK3 is also predicted to be a driver mutation based on biostatistical analysis (8)). These results were verified using PMUT (16), and all three DAPK3 mutations were predicted to be driver mutations (pathological). To demonstrate that many of the mutations analyzed by CanPredict are suggested to be passenger mutations, we have included the analysis of RIPK1 (Figure 1C).

We generated the three observed DAPK3 somatic mutations - T112M (colon cancer (CRC)), D161N (ovarian cancer), and P216S (NSCLC) - in full-length DAPK3 cDNA using site-directed mutagenesis. FLAG-tagged versions were expressed in the H157 NSCLC cell line, which was selected for initial studies because it is amenable to transfection and is sensitive to apoptotic stimuli, and 293T cells. To assess kinase activity, we monitored phosphorylation of MLC2, a reported DAPK3 substrate (17), at T18/S19 by blotting with anti-pT18/pS19 antibodies. Expression of WT DAPK3 increased MLC2 phosphorylation (Figure 1D), whereas expression of D161N, T112M and P216S did not. These data suggest that all three somatic mutations inactivate DAPK3, since overexpression of the DAPK3 cancer mutants did not increase MLC2 phosphorylation. As a positive control we expressed the constitutively active  $\Delta 273$  DAPK3 mutant (ZIPK $\Delta 273$ ), which is a C-terminal truncation variant that consists of only the kinase domain and was previously reported to have increased kinase activity (18). As a negative control we expressed T180A DAPK3 (mutated at the key activation loop autophosphorylation site), which was reported to have decreased kinase activity (18). We complemented these studies by carrying out *in vitro* kinase assays with DAPK3 immunoprecipitated (IP) from H157 cells using recombinant GST-MLC2 purified from bacteria cells as a substrate (Figure 1E). Consistent with the *in vivo* results,

D161N, P216S, and T180A DAPK3 had very low kinase activity compared to WT DAPK3; T112M had significantly decreased activity. Combined, these data indicate that DAPK3 mutations identified in cancer patients significantly suppress the activity of the kinase.

To determine if the DAPK3 cancer mutations alter the function of the WT kinase, we transiently expressed them in H157 cells (transfection efficiency is 70–90%, based on gating GFP<sup>+</sup> cells, and overexpression of WT DAPK3 is approximately 3-fold based on image J densitometry) and monitored cell survival and cell cycle progression of the whole cell population. Overexpression of WT DAPK3 under high-serum (10% FBS) media conditions caused cells to accumulate in G1, resulting in an increase in the G1/S ratio (Figure 2A). This phenotype was more pronounced with DAPK3  $\Delta$ 273, but all three cancer-variants of DAPK3, as well as T180A were ineffective at inhibiting cell cycle progression. To determine if this inhibition of cell cycle progression translated into a decrease in cellular proliferation we overexpressed DAPK3 constructs in H157 cells and monitored BrdU incorporation. Consistent with the cell cycle analysis, overexpression of WT DAPK3 and the constitutively active  $\Delta$ 273 DAPK3 significantly decreased BrdU incorporation (Figure 2B), whereas the DAPK3 T180A mutant and all three cancer mutants did not (Figure 2B). These data are consistent with a model in which loss of functional growth inhibitory DAPK3 may increase cell proliferation, a hallmark of tumorigenesis.

To our knowledge this was the first time DAPK3 has been implicated in regulating cell cycle progression and proliferation. To verify that endogenous DAPK3 regulates the cell cycle we depleted endogenous DAPK3 from H157 NSCLC cells and U87 glioma cells, which both have WT DAPK3, using SMARTpool siRNA transfection. Immunoblots (IB) demonstrated that the level of endogenous DAPK3 was significantly reduced, correlating with a decrease in phosphorylation of downstream substrates, including histone H3 (T11) (19) and MLC2 (Thr18/Ser19) (Figure 2C left panel). In parallel, we measured relative BrdU incorporation in cells depleted of DAPK3, and found that this increased BrdU incorporation in both H157 and U87 cells (Figure 2C right panel), consistent with DAPK3 regulating both cell cycle progression and cell proliferation. To verify that the observed effect was not due to off-target effects, we depleted DAPK3 in H157 cells using DAPK3 specific single siRNA oligos. As displayed in Figure 2D, depletion of DAPK3 in the H157 cells correlated with a decrease in MLC2 phosphorylation as well as a decrease in the G1/S ratio indicating the cells are progressing through the cell cycle at an increased rate (Figure 2D).

To determine if DAPK3 regulated cell survival, we overexpressed DAPK3 constructs under low-serum conditions (0.1% FBS) and monitored apoptosis. Under these conditions, expression of WT DAPK3 caused a >2-fold increase in apoptosis, whereas expression of T112M, D161N, and P216S DAPK3 did not, again suggesting that these mutants are not functional (Figure 2E) (a similar increase in apoptosis is observed in these cells when treated with other cytotoxic agents such as etoposide, cis-platinum, or taxol (20)).

All the DAPK3 mutations identified to date in cancer patients are heterozygous, suggesting that a loss-of-function mutation in one allele could suppress the function of the WT allele by preventing activation of the WT allele following dimerization between an inactive DAPK3 cancer mutant and the WT DAPK3 proteins (15,18). To determine if these cancer mutants did indeed suppress the function of WT kinase, we first evaluated endogenous MLC2 phosphorylation in several cancer cell lines with high levels of phospho-MLC2 (T18/S19). Overexpression of WT DAPK3 (2–5 fold overexpression compared to endogenous DAPK3 based on Image J densitometry for the three cell lines examined) did not significantly increase MLC2 phosphorylation, although  $\Delta$ 273 DAPK3 did (Figure 3A). Consistent with the notion that the DAPK3 cancer mutants may suppress endogenous WT DAPK3 function,



overexpression of all three cancer-mutants as well as the T180A DAPK3 suppressed MLC2 phosphorylation. To verify that mutant endogenous DAPK3 could suppress WT DAPK3, we co-expressed the three cancer mutants individually with WT DAPK3 in H157 NSCLC cells and monitored phosphorylation of MLC2 (Figure 3B). Overexpression of WT DAPK3 increased MLC2 phosphorylation and this was blocked by coexpression of each of the cancer mutants when transfected at equal input DNA level (Figure 3B). To verify that the cancer mutants acted through association with WT DAPK3, we performed pull-down experiments with transiently coexpressed HA-tagged WT DAPK3 and FLAG-tagged WT DAPK3 or FLAG-tagged DAPK3 cancer mutants. Cancer mutants associated with WT DAPK3 to a level comparable to the WT DAPK3 (FLAG) (Figure 3C). Together these data suggest that the cancer mutants can act in a dominant manner to suppress the activity of the WT allele.

To determine if the DAPK3 cancer mutants could suppress the function of the WT kinase, we coexpressed T112M, D161N or P216S DAPK3 with WT DAPK3 in H157 NSCLC cells and monitored cell cycle progression. Coexpression of the cancer mutants caused a reduction in the G1/S ratio observed when WT DAPK3 is expressed alone (Figure 4A). This suggests that the cancer mutants interfere with the ability of WT DAPK3 to slow cell cycle progression. Consistent with these results, coexpression of DAPK3 cancer mutants with WT DAPK3 suppressed apoptosis induced by WT DAPK3 (Figure 4B). This provides further evidence that the cancer-associated mutations in DAPK3 exert a dominant-negative effect over WT DAPK3 function.

An important goal of this research is to address the functional relevance of mutations in cancer-associated kinases in the context of the cancer in which they occur. To this end we used a cell line, H1770, with an endogenous mutation in DAPK3 that occurred in a NSCLC patient, and was present in only the tumor cells. H1770 cells harbor a P216S mutation in DAPK3, which we have shown is a loss-of-function mutation (this cell line is heterozygous WT/P216S). Sequencing of DAPK3 RNA verified that H1770 cells carry the P216S endogenous mutation, and the sequencing chromatograms suggest that both alleles are expressed at equal levels (not shown). This NSCLC cell line is a suspension cell line that grows as large cellular aggregates (Figure 5A). Depletion of total DAPK3 from these cells with SMARTpool siRNA did not decrease MLC2 or histone H3 phosphorylation (levels of phosphorylation for these proteins were already very low and barely detectable with the antibodies (Figure 5C)), or alter cell cycle distribution, suggesting that DAPK3 and downstream signaling are inactive in this cell line (data not shown). Reconstitution of these cells with WT DAPK3 resulted in decreased cellular aggregation (Figure 5A, quantified in Figure 5B) and an increase in MLC2 phosphorylation (Figure 5C). Similar results were observed in cells expressing  $\Delta 273$  DAPK3 (Figure 5A and 5C), whereas no significant changes were observed in cells expressing P216S DAPK3. This suggests that loss of DAPK3 may enhance cellular aggregation and cell-to-cell adherence. Since cell-to-cell adhesion can promote chemotherapeutic resistance, we next determined if reconstitution of H1770 cells with WT DAPK3 rendered them more sensitive to chemotherapy. As shown in Figure 5D, cells expressing WT DAPK3 were somewhat more sensitive to etoposide than cells transfected with empty vector or P216S DAPK3. These data underscore the importance of the P216S mutation in this cell line, as reactivation of the DAPK3 pathway decreased cellular aggregation and rendered these cells more sensitive to apoptosis.

## Discussion

DAPK3 is a member of the death-associated protein kinase family and regulates cellular processes, including apoptosis, adherence, and cell cycle progression/proliferation (21). Several substrates have been reported for DAPK3, including MLC2, histone H3, and Par4

(9), and these substrates are likely to be important for DAPK3-mediated regulation of cell survival and cell cycle progression. DAPK3 has been suggested to be a tumor suppressor (21), and our results strongly implicate DAPK3 as a tumor suppressing kinase. In vitro and in vivo kinetic assays reveal that mutations in DAPK3 abolish or significantly reduce the enzymatic activity of DAPK3. Furthermore, we show that the DAPK3 cancer mutants are unable to inhibit cellular processes, including cell proliferation, demonstrating that these are loss-of-function mutations and suggesting that acquisition of these mutations by cancer cells will confer selective proliferative or survival advantages.

Previous reports have given us mechanistic insight into DAPK3 regulation and provide evidence that inactive DAPK3 forms a symmetrical homodimer through activation loop strand exchange between subunits (15,18). The kinase domain of DAPK3 is critical for the homodimerization and alone is sufficient to interact with full length DAPK3 (18). We present data showing that inactive DAPK3 proteins expressed from a mutant allele could act in a dominant-negative fashion by binding to WT DAPK3 and preventing its activation by T180 transphosphorylation (15). The data presented provide a mechanism where mutations observed in cancer may not only abolish the activity of the mutant allele, but may also act to suppress the function of the WT allele.

To determine if DAPK3 loss-of-function mutations confer an advantage in the context of a tumor where the mutation was acquired, we sought to reconstitute the H1770 NSCLC cell line with WT DAPK3 and monitor phenotypic effects. Interestingly expression of DAPK3 in the H1770 cell line resulted in a decrease in cellular aggregation, consistent with a loss of cell-to-cell adhesion that is likely to occur following MLC2 phosphorylation. Interestingly other MLC2 kinases are also mutated in this cell line (MYLK2 (A117V) and CDC42BPA (MRCK, E50K)) and the functional consequences of these mutations have not been determined. If these mutations were loss of function mutations, it would suggest a decrease in MLC2 phosphorylation (at both Ser 19 and Thr 18) was a critical step in the evolution of the tumor and potentially explains why increasing MLC2 phosphorylation at T18/S19 would have dramatic phenotypic consequences. Additionally, this observation may provide a novel insight into a pathway that could drive increased proliferation and drug resistance and could be a common pathway utilized to promote tumorigenesis. Cell-to-cell adhesion has previously been demonstrated to promote drug resistance, and, consistent with this observation, H1770 cells expressing wild-type DAPK3, which promotes loss of cell-to-cell adhesion, are more sensitive to chemotherapy (22). However, the role MLC2 phosphorylation in tumor formation is likely to be much more complex, and indeed activating mutations in ROCK1 have been described and increased MLC2 phosphorylation is also likely to play a critical role in tumor progression and increased migration (23). Interestingly one ROCK1-activating mutation described in the study by Lochhead et al., P1193S, which lies in the PH domain, was shown to be an activating mutation (22), and this mutation is also present in the H1770 cell line. The previous report did not examine MLC2 phosphorylation in H1770 cells, and our data suggest that overall MLC2 phosphorylation in these cells is barely detectable. It could be that this mutation promotes an increase in phosphorylation of another ROCK1-specific substrate or a small pool of MLC2. Comparing the various ROCK1 mutations evaluated in this study indicates that the P1193S did not appear to increase MLC2 phosphorylation significantly above WT ROCK1 and much less than the other two activating mutations. Additionally, P1193S ROCK1 appeared to have a unique cellular localization, and this could be due to a structural change in the PH domain induced by the mutation. Different consequences of MLC2 phosphorylation at S19 and combined phosphorylation at T18/S19 may contribute to the complex results.

Consistent with our general hypothesis, recent revelations have demonstrated that decreased MLC2 phosphorylation may promote tumorigenesis (24). Specifically, loss-of-function

mutations in LKB1 should lead to decreased NUA1 activation, resulting in decreased inhibition of the MLC2 phosphatase, MYPT1, due to decreased 14-3-3 binding (24). MYPT1 would then be free to dephosphorylate MLC2 and maintain it in a dephosphorylated state (24). In agreement with this hypothesis, MCF-10A cells depleted of LKB1 grow as abnormally large acini with multi-layering of acinar cells (25). Loss-of-function mutations in DAPK3 would be another mechanism to promote decreased MLC2 phosphorylation. Interestingly, the H157 NSCLC cell line has a loss-of-function mutation in LKB1, and this cell line is very responsive to increases in MLC2 phosphorylation, likely because phosphorylation of the substrate is normally suppressed by increased MYPT1 activity (26). Thus loss-of-function mutations in either LKB1 or DAPK3 could lead to suppression of MLC2 phosphorylation, promote cell-to-cell adhesion and lead to increased drug resistance (Figure 5D). Drugs that could promote MLC2 phosphorylation (or possibly diphosphorylation at T18/S19) could be valuable in the clinic in combination with other chemotherapeutics, particularly in patients with DAPK3 or LKB1 mutations, or decreased DAPK3 expression, such as in gastric cancer, where a recent study showed 111/162 gastric carcinomas displayed decreased expression of DAPK3, which was associated with increased metastasis and invasion (27).

## Summary

Cancer genomic studies that identify somatic mutations acquired in cancer cells will provide a roadmap for the identification and characterization of new oncogenes and tumor suppressors (28). These screens uncover mutations in known tumor-suppressing kinases, such as LKB1 and ATM, verifying the ability of these screens to identify mutationally inactivated tumor suppressors (8). Functional analysis of the consequences of cancer-associated mutations in signaling proteins, such as protein kinases, will lead to a broader understanding of signaling networks that contribute to tumorigenesis and define new targets that regulate these crucial networks. Combining the genomic screens with evolving and improving bioinformatics screens will provide a platform for basic researchers to identify new critical regulators of tumorigenesis that have a lower frequency of mutations, yet are still essential for tumorigenesis. The results presented illustrate the potential of this approach and suggest that DAPK3 is a tumor suppressor with loss-of-function mutations in cancer patients.

## Acknowledgments

This work was supported by Cancer Research UK (JB), American Cancer Society Postdoctoral Grant (#116653, JB), NCI Training Grant (#T32 CA009523 JB), US Public Health Service Grants CA14195 and CA82683 from the NCI (TH), and a sanofi-aventis Discovery grant (TH). TH is a Frank and Else Schilling American Cancer Society Professor.

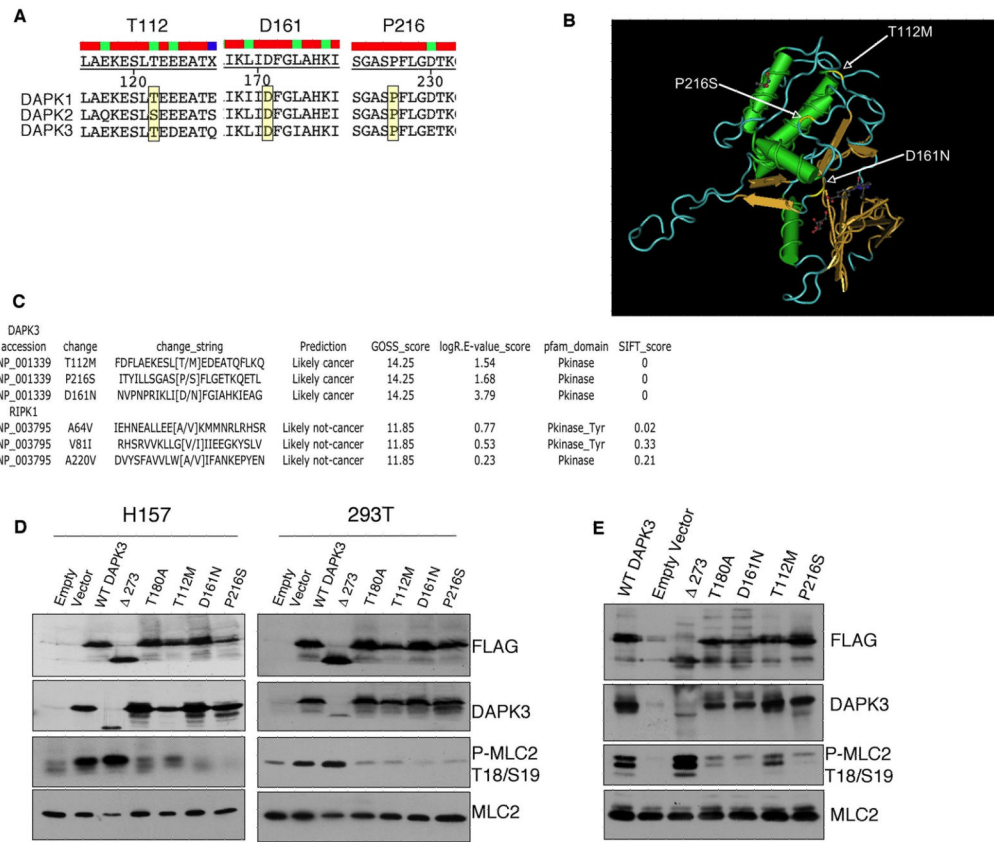
## References

1. Bonetta L. Whole-genome sequencing breaks the cost barrier. *Cell*. 141:917–9. [PubMed: 20550926]
2. Futreal PA, Coin L, Marshall M, et al. A census of human cancer genes. *Nat Rev Cancer*. 2004; 4:177–83. [PubMed: 14993899]
3. Boland CR, Goel A. Somatic evolution of cancer cells. *Semin Cancer Biol*. 2005; 15:436–50. [PubMed: 16055343]
4. Stuart D, Sellers WR. Linking somatic genetic alterations in cancer to therapeutics. *Curr Opin Cell Biol*. 2009; 21:304–10. [PubMed: 19328671]
5. Ferrer-Costa C, Gelpi JL, Zamakola L, Parraga I, de la Cruz X, Orozco M. PMUT: a web-based tool for the annotation of pathological mutations on proteins. *Bioinformatics*. 2005; 21:3176–8. [PubMed: 15879453]

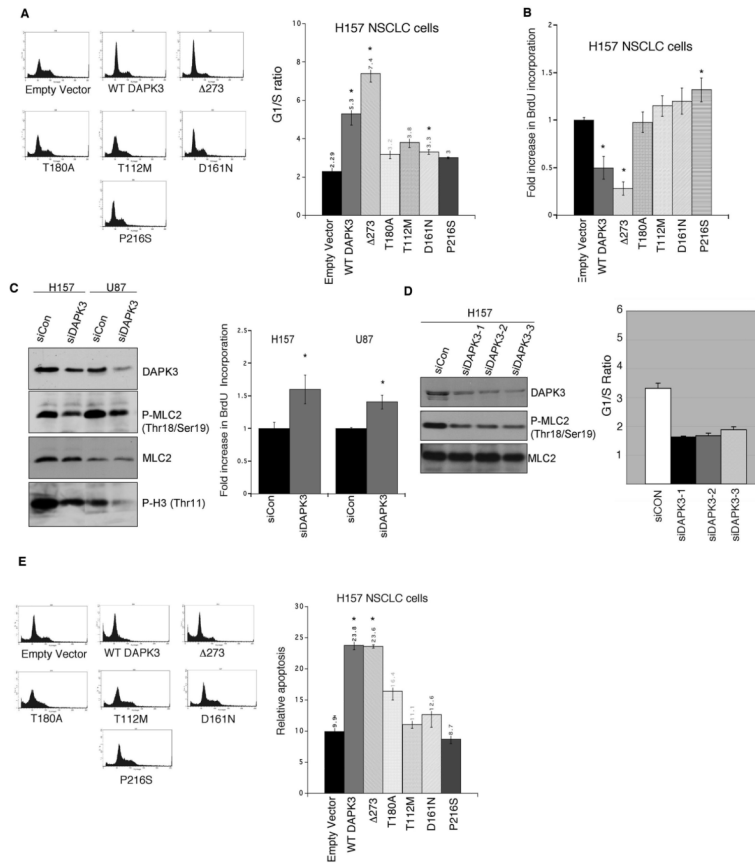


6. Kaminker JS, Zhang Y, Watanabe C, Zhang Z. CanPredict: a computational tool for predicting cancer-associated missense mutations. *Nucleic Acids Res.* 2007; 35:W595–8. [PubMed: 17537827]
7. Kaminker JS, Zhang Y, Waugh A, et al. Distinguishing cancer-associated missense mutations from common polymorphisms. *Cancer Res.* 2007; 67:465–73. [PubMed: 17234753]
8. Greenman C, Stephens P, Smith R, et al. Patterns of somatic mutation in human cancer genomes. *Nature.* 2007; 446:153–8. [PubMed: 17344846]
9. Bialik S, Kimchi A. The death-associated protein kinases: structure, function, and beyond. *Annu Rev Biochem.* 2006; 75:189–210. [PubMed: 16756490]
10. Detjen KM, Brembeck FH, Welzel M, et al. Activation of protein kinase Calpha inhibits growth of pancreatic cancer cells via p21(cip)-mediated G(1) arrest. *J Cell Sci.* 2000; 113 ( Pt 17):3025–35. [PubMed: 10934041]
11. Kawai T, Matsumoto M, Takeda K, Sanjo H, Akira S. ZIP kinase, a novel serine/threonine kinase which mediates apoptosis. *Mol Cell Biol.* 1998; 18:1642–51. [PubMed: 9488481]
12. Raval A, Tanner SM, Byrd JC, et al. Downregulation of death-associated protein kinase 1 (DAPK1) in chronic lymphocytic leukemia. *Cell.* 2007; 129:879–90. [PubMed: 17540169]
13. Rossi D, Gaidano G, Gloghini A, et al. Frequent aberrant promoter hypermethylation of O6-methylguanine-DNA methyltransferase and death-associated protein kinase genes in immunodeficiency-related lymphomas. *Br J Haematol.* 2003; 123:475–8. [PubMed: 14617009]
14. Ng MH, To KW, Lo KW, et al. Frequent death-associated protein kinase promoter hypermethylation in multiple myeloma. *Clin Cancer Res.* 2001; 7:1724–9. [PubMed: 11410512]
15. Pike AC, Rellos P, Niesen FH, et al. Activation segment dimerization: a mechanism for kinase autophosphorylation of non-consensus sites. *EMBO J.* 2008; 27:704–14. [PubMed: 18239682]
16. Ferrer-Costa C, Gelpi JL, Zamakola L, Parraga I, de la Cruz X, Orozco M. PMUT: a web-based tool for the annotation of pathological mutations on proteins. *Bioinformatics.* 2005; 21:3176–8. [PubMed: 15879453]
17. Murata-Hori M, Fukuta Y, Ueda K, Iwasaki T, Hosoya H. HeLa ZIP kinase induces diphosphorylation of myosin II regulatory light chain and reorganization of actin filaments in nonmuscle cells. *Oncogene.* 2001; 20:8175–83. [PubMed: 11781833]
18. Graves PR, Winkfield KM, Haystead TA. Regulation of zipper-interacting protein kinase activity in vitro and in vivo by multisite phosphorylation. *J Biol Chem.* 2005; 280:9363–74. [PubMed: 15611134]
19. Preuss U, Landsberg G, Scheidtmann KH. Novel mitosis-specific phosphorylation of histone H3 at Thr11 mediated by Dlk/ZIP kinase. *Nucleic Acids Res.* 2003; 31:878–85. [PubMed: 12560483]
20. Brognard J, Clark AS, Ni Y, Dennis PA. Akt/protein kinase B is constitutively active in non-small cell lung cancer cells and promotes cellular survival and resistance to chemotherapy and radiation. *Cancer Res.* 2001; 61:3986–97. [PubMed: 11358816]
21. Gozuacik D, Kimchi A. DAPk protein family and cancer. *Autophagy.* 2006; 2:74–9. [PubMed: 17139808]
22. Westhoff MA, Zhou S, Bachem MG, Debatin KM, Fulda S. Identification of a novel switch in the dominant forms of cell adhesion-mediated drug resistance in glioblastoma cells. *Oncogene.* 2008; 27:5169–81. [PubMed: 18469856]
23. Lochhead PA, Wickman G, Mezna M, Olson MF. Activating ROCK1 somatic mutations in human cancer. *Oncogene.* 29:2591–8. [PubMed: 20140017]
24. Zagorska A, Deak M, Campbell DG, et al. New roles for the LKB1-NUAK pathway in controlling myosin phosphatase complexes and cell adhesion. *Sci Signal.* 3:ra25. [PubMed: 20354225]
25. Partanen JJ, Nieminen AI, Makela TP, Klefstrom J. Suppression of oncogenic properties of c-Myc by LKB1-controlled epithelial organization. *Proc Natl Acad Sci U S A.* 2007; 104:14694–9. [PubMed: 17766436]
26. Zhong D, Guo L, de Aguirre I, et al. LKB1 mutation in large cell carcinoma of the lung. *Lung Cancer.* 2006; 53:285–94. [PubMed: 16822578]
27. Bi J, Lau SH, Hu L, et al. Downregulation of ZIP kinase is associated with tumor invasion, metastasis and poor prognosis in gastric cancer. *Int J Cancer.* 2009; 124:1587–93. [PubMed: 19117059]

28. Brognard J, Hunter T. Protein kinase signaling networks in cancer. *Curr Opin Genet Dev.* 2010 Nov 29. [Epub ahead of print].
29. Gao T, Furnari F, Newton AC. PHLPP: a phosphatase that directly dephosphorylates Akt, promotes apoptosis, and suppresses tumor growth. *Mol Cell.* 2005; 18:13–24. [PubMed: 15808505]



**Figure 1.** Mutational analysis and biochemical characterization of DAPK3 cancer variants. **A**, Sequence alignment of DAPK family members highlighting conservation of mutated residues in all three family members. Yellow boxes indicate amino acids mutated in cancer. **B**, Crystal structure of DAPK3 indicating where the mutations occurred. **C**, CanPredict analysis to demonstrate how this enhances the selection of putative cancer-associated kinases, the kinase RIPK1, which is predicted to have a driver mutation is not predicted to have a cancer-related mutation and therefore is not a good candidate for further investigation. In contrast, evaluation of somatic mutations of DAPK3 (also predicted to possess a driver mutation (99%)) reveal that all three somatic mutations are predicted to be cancer-related. **D**, H157 and 293T cells were transfected with vector or indicated FLAG-tagged DAPK3 constructs for 48 hr under high serum conditions prior to lysis. Immunoblots of lysates from H157 NSCLC or 293T cells were probed with antibodies to phospho-MLC2, MLC2, ZIPK, or anti-FLAG. **E**, H157 cells were transfected with vector or FLAG-tagged DAPK3 constructs as indicated under high serum conditions (10% FBS DMEM); thereafter FLAG-DAPK3 was immunoprecipitated and incubated with MLC2 generated from bl-21 bacterial cells. MLC2 phosphorylation was detected using phospho-specific MLC2 (Thr18/Ser19) antibodies.

**Figure 2.**

Mutations in DAPK3 result in loss-of-function. **A**, H157 NSCLC cells were transfected with indicated DAPK3 variants or vector alone, under high serum conditions (10% FBS DMEM) for 48 hr and apoptosis (sub-2N DNA content) and G1/S ratios were determined by propidium iodide incorporation assays and flow cytometry. An increase was observed in the G1/S ratio in cells transfected with FLAG-DAPK3 or FLAG-Δ273 compared to cells transfected with vector alone, T180A or cancer variants. Asterisks indicate p values less than 0.01. **B**, Overexpression of FLAG-DAPK3 or FLAG-Δ273 for 48 hr under high serum conditions decreased BrdU incorporation in H157 cells, whereas T180A or cancer mutants did not significantly alter BrdU incorporation. Asterisks indicate  $p < 0.05$ . **C**, Depletion of DAPK3 for 48 hr under high serum conditions increased BrdU incorporation in H157 and U87 cells. Immunoblots were performed in parallel to ensure that DAPK3 was being adequately depleted and we observed a concomitant decrease in MLC2 and histone H3 phosphorylation. Asterisks indicate  $p < 0.05$ . **D**, Depletion of DAPK3 with three unique siRNAs for 48 hr under high serum conditions decreased the G1/S ratio in the H157 cells. Immunoblots were performed in parallel to ensure that DAPK3 was being depleted. **E**, H157 cells were transfected with indicated constructs for 48 hr under low serum conditions. Histograms show sub-2N DNA; quantitation of sub-2N DNA is indicated in bar graph. Asterisks indicate  $p < 0.01$ . For all panels in Figure 2 the data in the bar graphs are representative of assays performed in triplicate, with error bars indicating standard deviation, and are representative of three independent experiments.

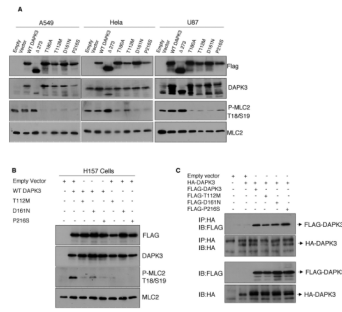


**Figure 3.** DAPK3 cancer mutants inhibit the activity of the wild type kinase. **A**, A549, HeLa, and U87 cells were transfected with the indicated constructs for 48 hr under high serum conditions prior to lysis. The phosphorylation state of MLC2 in lysates was detected by immunoblot analysis. **B**, Co-expression of cancer mutants suppresses the activity of WT DAPK3. H157 cells were co-transfected with the indicated constructs for 48 hr under high serum conditions and MLC2 phosphorylation was detected by immunoblot analysis. **C**, Cancer mutants associate with WT DAPK3. H157 cells were co-transfected with the indicated constructs for 48 hr under high serum conditions, lysed, immunoprecipitated overnight at 4 ° C, and association was detected by immunoblot analysis.



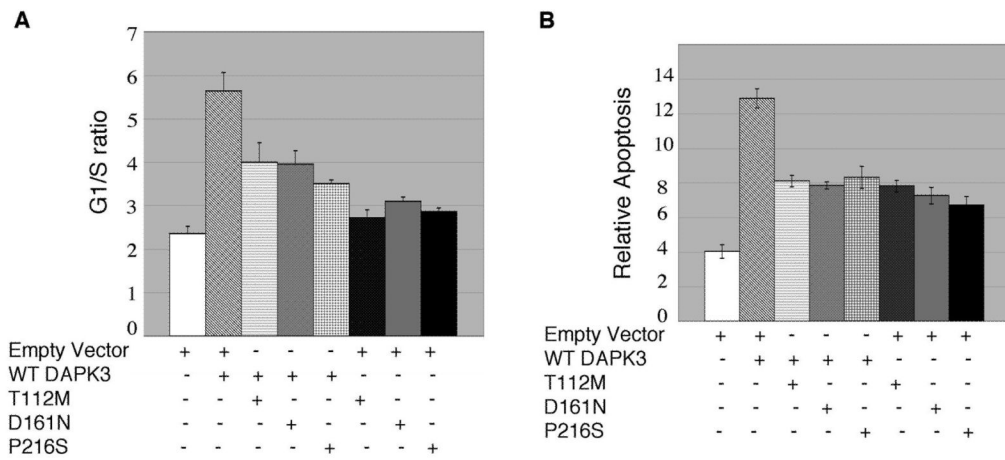


**Figure 4.** DAPK3 cancer mutants inhibit the function of the wild type kinase. **A, B** Co-expression of cancer mutants suppresses the function of WT DAPK3. H157 cells were co transfected with indicated constructs for 48 hr under high serum (10% FBS) (cell cycle analysis) or low serum (0.1% FBS) (apoptosis analysis) conditions. Apoptosis (sub-2N DNA content) and G1/S ratios were determined by propidium iodide incorporation assays and flow cytometry.

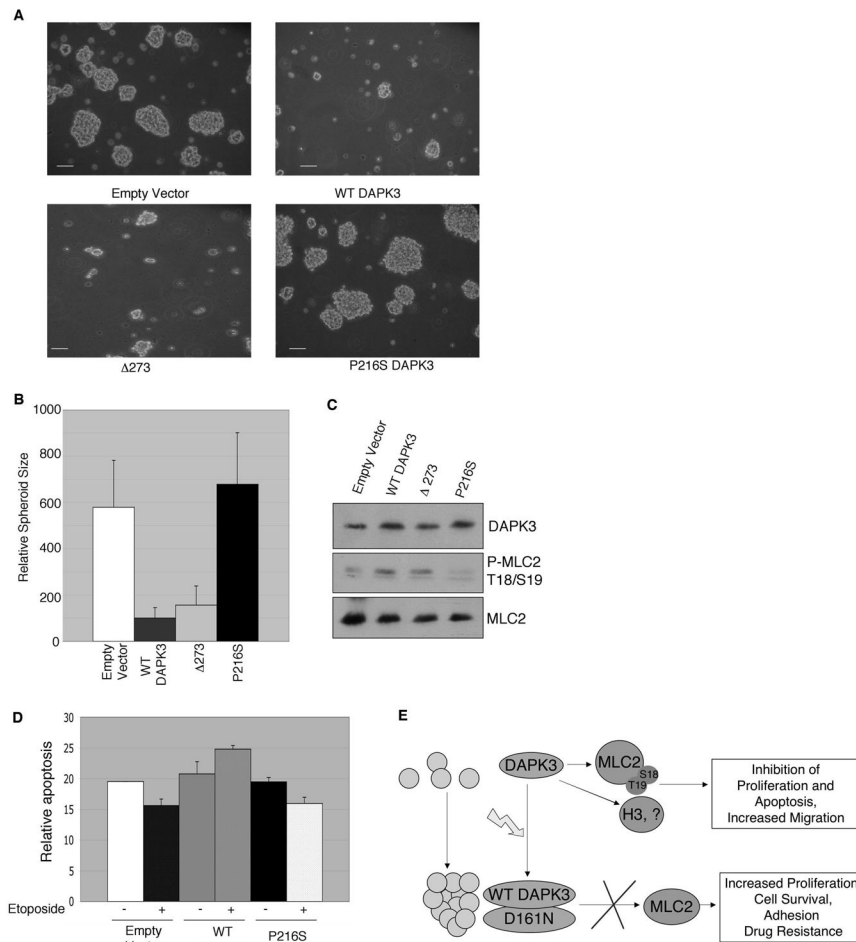


**Figure 5.** LOF mutation in DAPK3 promotes cell-cell adhesion and chemotherapeutic resistance. **A**, Reconstitution of DAPK3 pathway in H1770 cells that harbor a P216S mutation in DAPK3 reduces cell-cell adhesion. H1770 cells were transfected with the indicated constructs for 48 hr under high serum conditions and cells were photographed. White bar indicates 0.2 mm. **B**, Quantification of cellular aggregates is displayed and was determined using image J software based on the area occupied by a single cellular aggregate. **C**, Cells were then harvested, lysed, and immunoblot analysis was performed. **D**, H1770 cells expressing WT DAPK3 are more sensitive to etoposide-induced apoptosis. Cells were transfected with WT or cancer mutant P216S DAPK3, maintained in low serum growth media (0.1% FBS) and treated with vehicle or 50  $\mu$ M etoposide for 48 hr prior to harvesting cells and determining sub-2N DNA content by propidium iodide incorporation assays and flow cytometry. **E**, Model depicting results of loss of function mutation of DAPK3 promotes increased adhesion, survival, proliferation, and promotes drug resistance.